Mon. Not. R. Astron. Soc. 280, L19–L26 (1996)

Non-linear evolution of cosmological power spectra

J. A. Peacock[1] and S. J. Dodds[2]

[1]Royal Observatory, Blackford Hill, Edinburgh EH9 3HJ
[2]Institute for Astronomy, University of Edinburgh, Blackford Hill, Edinburgh EH9 3HJ

Accepted 1996 March 12. Received 1996 March 12; in original form 1996 January 12

ABSTRACT

Hamilton et al. have suggested an invaluable scaling formula which describes how the power spectra of density fluctuations evolve into the non-linear regime of hierarchical clustering. This paper presents an extension of their method to low-density universes and universes with non-zero cosmological constant. We pay particular attention to models with large negative spectral indices, and give a spectrum-dependent fitting formula which is of significantly improved accuracy by comparison with an earlier version of this work. The tendency of non-linear effects to increase power on small scales is stronger for spectra with more negative spectral indices, and for lower densities. However, for low-density models with a cosmological constant, the non-linear effects are less strong than for an open universe of the same Ω.

Key words: cosmology: theory – large-scale structure of Universe.

1 INTRODUCTION

The power spectrum of density fluctuations is a statistic of central importance in cosmology, as it describes a combination of the primordial deviations from homogeneity and their subsequent modification by the matter content of the universe. One practical obstacle to a measurement of this useful function is that the present universe occupies a state where non-linear gravitational growth of density fluctuations has altered the form of the fluctuation spectrum.

Prior to 1991, it was assumed that this problem was tractable only in two extreme limits. On large scales, linear theory applies and the power spectrum scales as the square of the density growth factor. For very large wavenumbers, we enter the 'stable clustering' regime, where there is a simple relation between the power-law index of the spectrum and that of the output non-linear spectrum (see section 73 of Peebles 1980). It was therefore a significant breakthrough when Hamilton et al. (1991, hereafter HKLM) suggested a scaling procedure which allowed an accurate description of the transition regime between these two limits in terms of an empirical universal function.

In a previous paper (Peacock & Dodds 1994, hereafter PD), we extended the HKLM procedure in a number of ways. First, we presented a version of the method which worked with power spectra, rather than HKLM's choice of integrated correlation function. Secondly, we considered the modifications to the HKLM argument needed to work in a universe of arbitrary density, rather than HKLM's $\Omega=1$. We applied this extended HKLM method to a compilation of clustering data, and concluded that the linearized data for $k \lesssim 0.4h$ Mpc^{-1} ($h \equiv H_0/100$ km s^{-1} Mpc^{-1}) were consistent with a spectral index of about -1.5 on small scales, steepening to close to the primordial $n=1$ on large scales [$P(k) \propto k^n$].

However, the universal scaling procedure of HKLM was known to fail for more negative spectral indices, as has been investigated in some detail recently for $\Omega=1$ models by Jain, Mo & White (1995, hereafter JMW). A common description of the linear power spectrum is in terms of the cold dark matter (CDM) model, whose power-law slope tends to -3 on very small scales, so the HLKM method and its extensions in PD may not work very well if we attempt to investigate scales significantly smaller than those studied in PD. We have therefore run an additional ensemble of N-body simulations which concentrate on the case of spectra with $n \lesssim -1$ and the CDM spectrum. It turns out that a simple slope-dependent correction can be made to the PD formulae which provides an excellent description of the non-linear data over essentially all regimes of interest, and this is described below.

2 THE HKLM METHOD

The key argument of HKLM is that gravitational collapse causes a change of scale. By regarding the integrated correlation function $\bar{\xi}(r)$ as measuring the number of excess neighbours within radius r, they suggested that observed non-linear correlations on non-linear scale $r_{\rm NL}$ be related to a pre-collapse linear scale via

$$r_{\rm L}=[1+\bar{\xi}_{\rm NL}(r_{\rm NL})]^{1/3}r_{\rm NL}. \tag{1}$$

HKLM then conjectured that, having translated scale, the linear and non-linear correlations had some universal relation

$$\bar{\xi}_{\rm NL}(r_{\rm NL})=f_{\rm NL}[\bar{\xi}_{\rm L}(r_{\rm L})]. \tag{2}$$

The function $f_{\rm NL}$ must behave as $f_{\rm NL}(x)=x$ in the linear $x\ll 1$ limit and $f_{\rm NL}(x)\propto x^{3/2}$ in the stable-clustering $x\gg 1$ limit, and must be determined numerically around $x\sim 1$.

PD argued that a very similar argument could be made to work for power spectra, using a dimensionless version of the power spectrum: Δ^2 is the contribution to the fractional density variance per unit $\ln k$. In the convention of Peebles (1980), this is

$$\Delta^2(k)\equiv\frac{{\rm d}\sigma^2}{{\rm d}\ln k}=\frac{V}{(2\pi)^3}4\pi k^3|\delta_k|^2 \tag{3}$$

(V being a normalization volume), and the relation to the correlation function is

$$\xi(r)=\int\Delta^2\frac{{\rm d}k}{k}\frac{\sin kr}{kr}. \tag{4}$$

Since $\bar{\xi}(r)$ can be thought of as Δ^2 at some effective wavenumber, this suggests the k-space version of HKLM:

$$k_{\rm L}=[1+\Delta^2_{\rm NL}(k_{\rm NL})]^{-1/3}k_{\rm NL}, \tag{5}$$

$$\Delta^2_{\rm NL}(k_{\rm NL})=f_{\rm NL}[\Delta^2_L(k_{\rm L})]. \tag{6}$$

The extension to models with $\Omega\neq 1$ is straightforward in the highly non-linear regime. The $f_{\rm NL}(x)\propto x^{3/2}$ scaling comes because, once a virialized object is formed, the non-linear correlations depend on scalefactor $a(t)$ just as a background density, $\bar{\xi}_{\rm NL}\propto a^3$, whereas the linear correlations scale as $\bar{\xi}_{\rm L}\propto a^2$. If we now allow a density-dependent growth-suppression factor into the linear growth law,

$$\bar{\xi}_{\rm L}\propto[ag(\Omega)]^2, \tag{7}$$

the virialized regime becomes

$$f_{\rm NL}(x)\propto x^{3/2}[g(\Omega)]^{-3}. \tag{8}$$

The $g(\Omega)$ factor may conveniently be taken from the high-accuracy fitting formula of Carroll, Press & Turner (1992):

$$g(\Omega)=\frac{5}{2}\Omega_{\rm m}[\Omega_{\rm m}^{4/7}-\Omega_{\rm v}+(1+\Omega_{\rm m}/2)(1+\Omega_{\rm v}/70)]^{-1}, \tag{9}$$

where we have distinguished matter (m) and vacuum (v) contributions to the total density parameter.

The problem is now reduced to one of running a number of N-body simulations to obtain the full form of $f_{\rm NL}$ and to investigate its dependence on the cosmological model. The power of the original HKLM method was the belief that $f_{\rm NL}$ was a universal function. Using this assumption, PD fitted a g-dependent non-linear function to a restricted set of N-body simulations – a procedure which works reasonably well for spectra with n in the region of -1. With the larger library of simulations studied here, however, it is possible to see that there is a dependence on the linear spectrum, but one that can be described well by a simple fitting formula.

3 NUMERICAL DATA AND FITS

3.1 *N*-body code

The carrying out of the required set of numerical experiments has become much easier recently, partly owing to an increase in the power of computer hardware, but mainly through the generous distribution of the Adaptive Particle–Particle–Particle Mesh (AP3M) code of Couchman (1991). This solves the Poisson equation on a mesh to obtain the large-scale force, which is then supplemented by exact pairwise forces from the near neighbours. Such P3M codes normally slow down for highly clustered distributions, but this is avoided in Couchman's method by adaptive regridding of the densest regions on a finer mesh.

For the present purposes, the main problem with Couchman's code is that it is supplied for an $\Omega=1$ cosmology only. The equations of motion use positions, x, measured in units of the box size, $L_{\rm box}$ (plus a scaling with the Fourier mesh size). The velocities are defined with these length units and a time unit of the age of the universe at the start of the simulation. Also, a 'time' variable, p, is used to integrate the equations of motion:

$$p=\frac{3}{2\alpha}a^{\alpha}. \tag{10}$$

In principle, the index α can be altered according to the spectrum; we retained $\alpha=3/2$, so that both p and the scalefactor a were unity at the start of the simulation.

The standard equation of motion (e.g. section 14 of Peebles 1980) can then, with a little effort, be cast into the form (dashes denoting ${\rm d}/{\rm d}p$)

$$\boldsymbol{v}'+\left[\frac{1}{p}+\frac{2}{\alpha p}+\frac{T'}{T}\right]\boldsymbol{v}=\Omega_{\rm m}(p)\left(\frac{3}{2\alpha p}\right)^2\boldsymbol{f}, \tag{11}$$

where $\boldsymbol{f}$ is the force vector as calculated by the AP3M program, and $T=H(p)t_i$ is the product of the physical Hubble parameter and the initial time. The required modifications to the AP3M equations of motion are therefore to multiply the forces on the rhs by $\Omega_{\rm m}(p)$ and to use the appropriate $T(p)$. Note that a non-zero cosmological constant only enters through $T(p)$.

For an Einstein–de Sitter universe, $T=(2/3)a^{-3/2}$. In general, we have the exact result (Carroll et al. 1992)

$$H(a)=H_0\sqrt{\Omega_{\rm v}(1-a^{-2})+\Omega_{\rm m}(a^{-3}-a^{-2})+a^{-2}}. \tag{12}$$

There is also the excellent approximation

$$H_0t_0=\frac{2}{3}|1-f|^{-1/2}S_k\sqrt{\frac{|1-f|}{f}}, \tag{13}$$

where $f=0.7\Omega_{\rm m}-0.3\Omega_{\rm v}+0.3$ and S_k is sinh if $f<1$, otherwise sin. This is not needed, however, since we are only interested in T'/T:

$$\frac{T'}{T} = \frac{1}{2\alpha p} \frac{\Omega_m(2a^{-2} - 3a^{-3}) + 2a^{-2}\Omega_v - 2a^{-2}}{\Omega_m(a^{-3} - a^{-2}) + \Omega_v(1 - a^{-2}) + a^{-2}}. \tag{14}$$

The only problem with using these formulae to obtain $T(a)$ is Couchman's convention that the reference time t_0 at which $a = 1$ is at the start of the simulation, so that Ω_m and Ω_v in the above formulae are the initial values, not those at the desired endpoint of the simulation, designed to correspond to the present epoch. To relate the initial and final values of Ω_m and Ω_v, we use

$$\Omega_m(a) = \frac{\Omega_m}{a + \Omega_m(1 - a) + \Omega_v(a^3 - a)}, \tag{15}$$

$$\Omega_v(a) = \frac{a^3\Omega_v}{a + \Omega_m(1 - a) + \Omega_v(a^3 - a)}. \tag{16}$$

These formulae work whether $a = 1$ is regarded as the start or as the end of the simulation; the important thing is not to mix the conventions.

Lastly, there is the question of initial conditions. The AP3M program generates a realization of a displacement field corresponding to the given power spectrum. A possible source of confusion, as usual, lies in power-spectrum units. Couchman's function pow relates to the notation here via

$$\mathrm{pow} = \frac{2\pi^2}{[L_{\mathrm{box}}k]^3} \Delta^2(k). \tag{17}$$

Zeldovich initial conditions are assumed, so that initial displacement and velocity are proportional. However, in order to be properly in the growing mode, the $\Omega = 1$ velocities should be multiplied by the growth factor $\Omega_m^{0.6}$ (initial) (effectively independent of Ω_v: Lahav et al. 1991).

3.2 Simulations and analysis

There are many degrees of freedom in possible N-body runs. The physical ones are the power spectrum of interest and the cosmological model. The size of the simulation box also matters, since this must be set so that the fundamental mode does not saturate:

$$\Delta^2(2\pi/L_{\mathrm{box}}) \ll 1. \tag{18}$$

If this condition is violated, the results may not be reliable on any scale, owing to the missing power beyond the box-scale; we used a maximum value of 0.04. It is also necessary that Δ^2 on the initial mesh-scale does not exceed unity, so that the Zeldovich method used to set up initial conditions does not produce excessive shell crossing. For steep spectra, this can imply a more restrictive limit on the final box-scale amplitude.

There remain the numerical parameters of the number of particles, the total expansion factor, the number of time-steps, the force softening and the required force accuracy. We carried out various experiments varying these parameters, to see how robust the results were. We generally found that even quite simple simulations would reproduce the main features of the non-linear results here, particularly in the quasi-linear regime. We obtained most of our data in a standard configuration of $N = 80^3$ particles, integrated in 300 time-steps over an expansion factor of 15. A 128^3 Fourier mesh was used, with the initial softening set at one cell, held constant in proper terms down to a minimum of 0.1 cell. Some cases were checked in $N = 100^3$ runs with 600 time-steps, but these much longer simulations gave essentially identical results.

The only factors that influenced the resulting power spectra significantly were particle placement and the question of whether or not to use proper Gaussian realizations in the initial conditions. It is common to start N-body simulations by applying the initial displacement field to particles placed on a uniform grid, but there are times when this is not desirable. For example, the original grid is often noticeable even at late times in void regions. A cosmetic improvement can be made by starting from a set of particle positions which are irregular but subrandom, such as the 'glass' described by Baugh, Gaztañaga & Efstathiou (1995). A simpler alternative is to displace each particle randomly within its grid cell, which sets up an $n = 2$ spectrum of initial perturbations in addition to those imposed by the initial displacement field. With any of these alternatives, some care is needed when obtaining the power spectrum of the density field.

As in the case of redshift surveys, the particle distribution is Fourier analysed, and shot noise is subtracted from the raw power to allow for particle discreteness (see Peacock & Nicholson 1991). This would be a correct procedure at all times if the initial particle positions were also Poisson distributed, but the resulting small-scale fluctuations would then swamp the desired physical spectrum. The alternative starting schemes cure this problem, but introduce discreteness fluctuations that are initially smaller than Poisson, so that subtracting shot noise underestimates the spectrum in the early stages of the simulation. Small-scale mixing rapidly cures this problem at large k (effectively as soon as the first pancakes form), but the overall spectrum will not be correct until the large-scale portion has grown enough to exceed the shot power

$$\Delta^2_{\mathrm{shot}} = \frac{4\pi}{N} [k/(2\pi/L_{\mathrm{box}})]^3. \tag{19}$$

For $N = 80^3$ particles, the shot power on the box-scale is $\Delta^2_{\mathrm{shot}} = 10^{-4.6}$, and this only becomes negligible when the box-scale power is $\sim 10^{-3}$. For $n < 0$, the shot power rises more rapidly with k than the physical power, and so in practice larger values of the box-scale power need to be used in order that the quasi-linear part of the spectrum is not affected by shot-noise subtraction. For $n = -2$, this requires box-scale power at the non-linear limit of 0.04: simulation of more negative indices is not feasible without a great increase in the number of particles used.

Even for the analysis of $N \sim 10^6$ particles, only a fast Fourier transform (FFT) is practical, in which case the range of k accessible is limited by the size of the FFT array. For a 256^3 mesh (our normal limit), the Nyquist frequency is only 128 times the fundamental frequency, and even here the power spectrum is affected by binning and by aliasing (Baugh & Efstathiou 1994). The binning correction is, to second order in k,

$$\Delta^2_{\mathrm{bin}} = \Delta^2_{\mathrm{true}}/(1 + k^2B^2/12), \tag{20}$$

where B is the bin size (=simulation box/256). Aliasing effects depend on the slope of the power spectrum; gravitational instability tends to produce an effective index in the range -1 to -2, so this is not a problem in practice. Normally this size of FFT was sufficient for our purposes, but occasionally we wished to extend the results to smaller scales. We then divided the data into a set of subcubes and analysed each separately, obtaining an estimate of the small-scale power spectrum by averaging. Although these samples are individually quite non-linear on their box-scale, a few comparisons with time-consuming direct Fourier transforms of the complete data set indicated that the overall power spectrum could be recovered in this way over a factor of 300 in k, allowing the maximum range of non-linearity to be probed in a way consistent with the resolution of the simulations. It is interesting to note that great accuracy is required in the Fourier analysis. A small error in non-linear power produces a small error in the deduced linear power; however, because $f_{\rm NL}$ is so steep in the quasi-linear regime, this small horizontal shift can result in a gross vertical error in $f_{\rm NL}$. More comfortingly, this means that the forward prediction of non-linear power is quite robust with respect to moderate errors in $f_{\rm NL}$, and our simple parametrization of the numerical results should give very accurate results in most circumstances.

Finally, to create a proper realization of Gaussian initial perturbations, each Fourier mode should have a random phase and a power exponentially distributed about the mean. The alternative is to use exactly the expectation power, which has the advantage that the large-scale linear portion of the power spectrum does not suffer a large scatter owing to the limited number of modes. The results on intermediate and small scales seemed identical in either case, and so we used 'improper' realizations.

In this way, we built up a library of results covering $-2<n<0$ and $0.1<\Omega_{\rm m}<1$, considering both open models with $\Omega_{\rm v}=0$ and flat models with $\Omega_{\rm v}+\Omega_{\rm m}=1$. For the same cosmologies, we also considered CDM spectra, which are parametrized by the shape Ωh and the normalization σ_8 (see PD). For a given cosmology, these are degenerate degrees of freedom in that a reinterpretation of the simulation box length will change both Ωh and σ_8. It therefore suffices to fix one parameter and vary the other. We considered what is

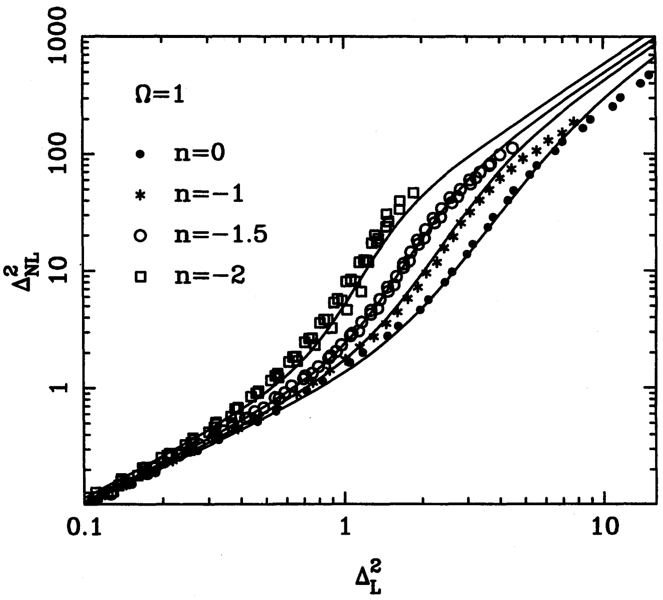

Figure 1. The generalized HKLM function relating non-linear power to linear power, for an $\Omega=1$ Einstein–de Sitter universe and power-law spectra with $n=0, -1, -1.5$ and -2. The solid lines show the fitting formula of Section 3.3. For spectra with $n \gtrsim -1$, the function shows very little spectral dependence. For flatter spectra, the non-linear power at a given linear power is higher; in particular the slope of the quasi-linear portion around $\Delta^2_{\rm NL}\sim 10$ increases as n decreases, from approximately $f_{\rm NL}(x)\propto x^3$ for $n=0$ to $f_{\rm NL}(x)\propto x^4$ for $n=-2$.

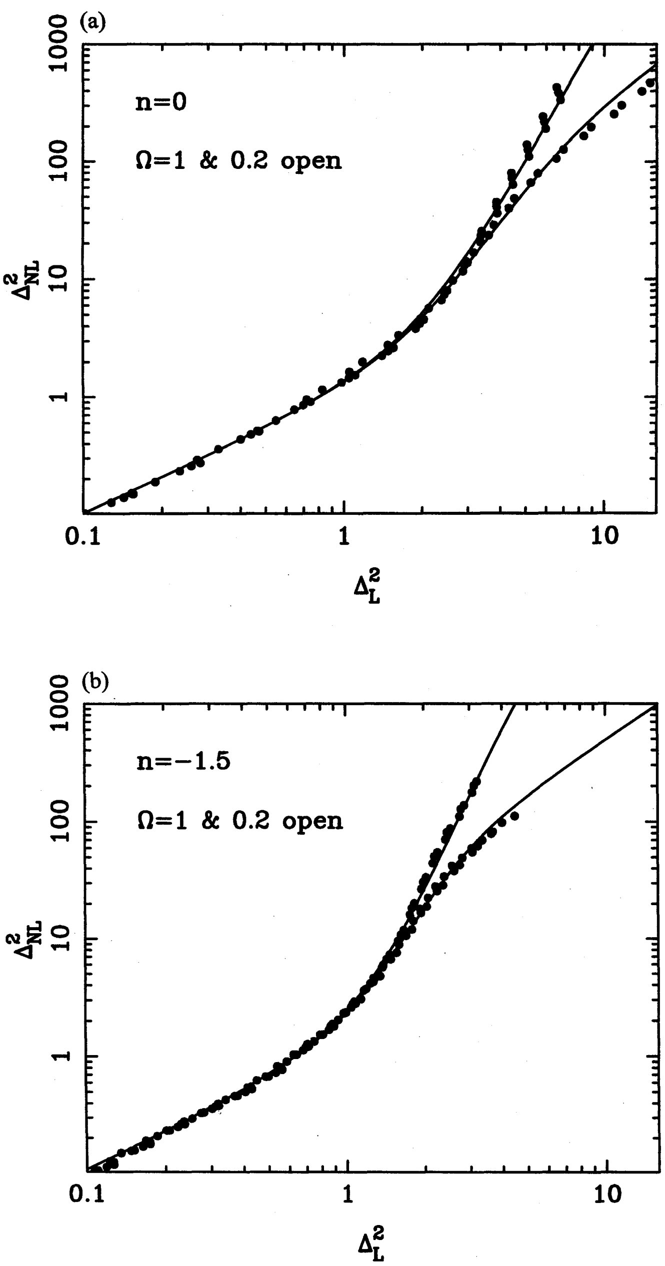

Figure 2. The generalized HKLM fnction relating non-linear power to linear power, for $\Omega_{\rm m}=1$ and 0.2 at zero vacuum energy. (a) An $n=0$ spectrum; (b) $n=-1.5$. The solid lines show the fitting formula of Section 3.3. As Ω decreases, the non-linear power increases and the quasi-linear portion steepens. However, these changes are largely associated with the increase of $f_{\rm NL}$ in the virialized regime with $\Delta^2_{\rm NL}\gtrsim 100$.

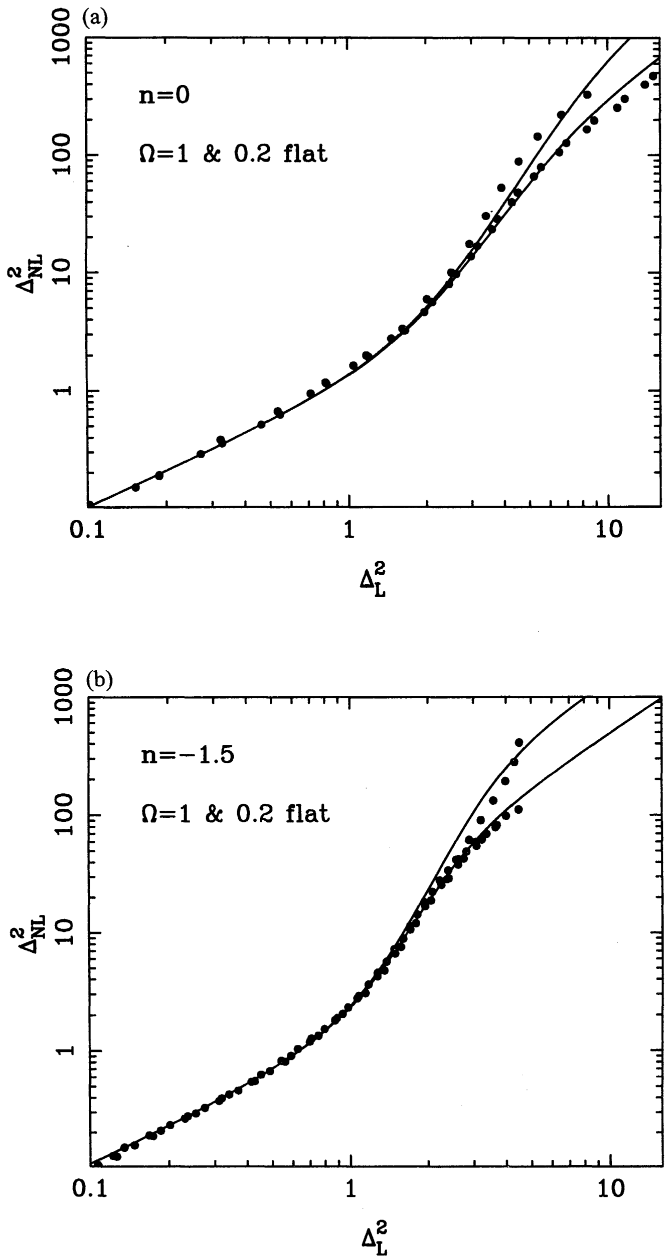

Figure 3. As for Fig. 2, but for spatially flat models with $\Omega_v + \Omega_m = 1$. The generalized HKLM function relating non-linear power to linear power, for $\Omega_m = 1$ and 0.2. (a) An $n = 0$ spectrum; (b) an $n = -1.5$ spectrum. The solid lines show the fitting formula of Section 3.3. The Ω dependence is weaker than for open models, consistent with the idea that all that matters is the growth-suppression factor $g(\Omega)$.

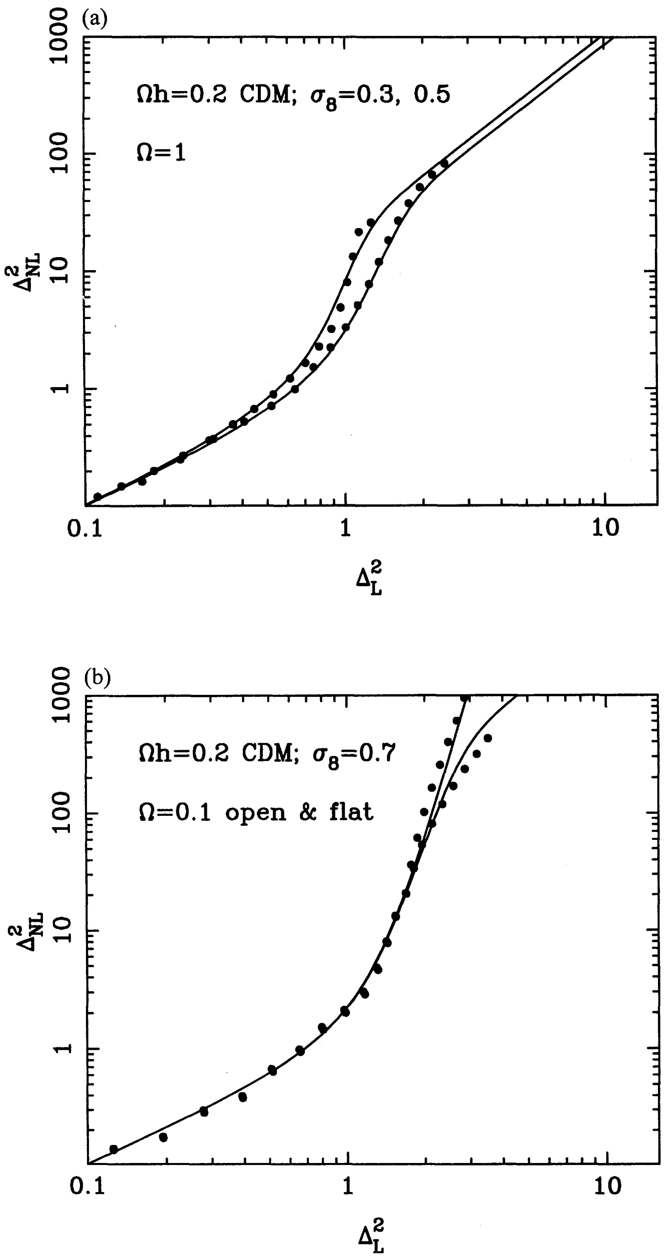

Figure 4. As for Fig. 2, but for standard CDM spectra. The generalized HKLM function relating non-linear power to linear power. (a) For an $\Omega = 1$ Einstein–de Sitter universe; $\Omega h = 0.2$ and $\sigma_8 = 0.3$ and 0.5. (b) For an $\Omega_m = 0.1$ universe with $\Omega_v = 0$ and 0.9; $\Omega h = 0.2$, $\sigma_8 = 0.7$. The solid lines show the fitting formula of Section 3.3. Note that the CDM curves are steeper even than the $n = -2$ power-law results, suggesting that the small-scale CDM behaviour is characteristic of the tangent spectral index there, which can be as negative as $n = -2.5$ for the models studied here. Fig. 4(b) shows clearly the extra small-scale power produced in the case of an open model by comparison with a flat model of the same Ω_m.

roughly the observed shape, $\Omega h = 0.2$, in a $100\,h^{-1}$ Mpc box, with final values of σ_8 in the range 0.4–1. For all these simulations, results are available in the form of both the final output time and earlier times. To be sure that the results were free from artefacts of the initial conditions, we used only the last factor of 2 expansion, since at least a factor of 3 expansion is required in order for initial transients to die down (Baugh et al. 1995). This gave a set of 48 determinations of f_{NL} to be fitted, from 18 distinct simulations.

The next few figures give a selection of results. Fig. 1 shows f_{NL} for a variety of power-law spectra with $\Omega = 1$, whereas Figs 2 and 3 show how these change with decreasing Ω, both without and with a cosmological constant. Figs 2 and 3 illustrate the point made by PD, that f_{NL} steepens as we go to lower-density models. Fig. 1 shows that JMW were correct in claiming that there was also a significant dependence on spectral index, particularly for spectra with $n \lesssim -1$. Such flat spectra have a larger f_{NL}, but f_{NL} also appears to steepen for more negative n, whereas JMW suggested a fit in which the slope of the quasi-linear portion was independent of n; in retrospect, this steepening can also be seen in their data. Interestingly, however, the spectrum dependence is less extreme for low-density models, as may be seen in Fig. 2: for low densities, the quasi-linear portion of $f_{\rm NL}$ has a similar slope for both $n=0$ and $n=-1.5$. This is an important hint as to how to achieve an improved fit to the results. What seems to be happening is that the main effect of changing the density is to alter the amplitude of the virialized $f_{\rm NL}(x)\propto x^{3/2}$ asymptote. JMW suggested that this amplitude was also a function of spectrum, being larger for $n=-2$ than for $n=0$ by about a factor of 2. This could account nicely for the different degrees of density-dependent steepening: for $n\simeq -2$, the asymptote is at a sufficiently high level that raising it still further by lowering the density has a small effect on the function. Conversely, for $n\simeq 0$, the non-linear function saturates quite early (for $\Omega=1$) owing to the low level of the asymptote. We now try to find a fitting formula to see how well this insight works quantitatively.

3.3 Fitting formula

The fitting formula has the same form as used by PD:

$$f_{\rm NL}(x)=x\left[\frac{1+B\beta x+[Ax]^{\alpha\beta}}{1+([Ax]^{\alpha}g^3(\Omega)/[Vx^{1/2}])^{\beta}}\right]^{1/\beta}. \qquad (21)$$

This contains five free parameters, each of which is potentially spectrum dependent. B describes a second-order deviation from linear growth; A and α parametrize the power-law which dominates the function in the quasi-linear regime; V is the virialization parameter which gives the amplitude of the $f_{\rm NL}(x)\propto x^{3/2}$ asymptote; β softens the transition between these regimes.

We proceeded by fitting the $\Omega=1$ results for individual power-law spectra, and looking at the trends of the parameters with n. This suggested a functional form which became progressively more non-linear as n approached -3 [as with the power of $(1+n/3)$ proposed by JMW]. The next step was to fit what is now a 10-parameter model to the data over the range $-2<n<0$, and this was achieved satisfactorily, with an overall rms accuracy of about 12 per cent in $f_{\rm NL}(x)$ over the range $0.1<\Delta^2_{\rm NL}<10^{2.5}$. Adding data with $\Omega\neq 1$ required very little alteration to the fit, as hoped from the discussion in the previous Section: the g^3 term in the fitting formula seems to be all that is required to incorporate different cosmological models.

The final step was to incorporate CDM results, which are important for two reasons. The CDM spectrum is the most important example of a spectrum which curves slowly so that the effective power-law index $n_{\rm eff}\equiv {\rm d}\ln P/{\rm d}\ln k$ varies with scale. It is also a useful case for the present investigation, since it contains very little large-scale power, but has an effective n that tends to -3 on small scales. Pure power-law spectra with $n<-2$ are very hard to simulate: being so flat, they tend to saturate the fundamental mode before enough small-scale non-linear evolution has occurred to erase the initial conditions. JMW suggested that the non-linear behaviour of CDM models could be modelled via the power-law model corresponding to $n_{\rm eff}$ at the non-linear scale. However, it seemed to us that the whole philosophy of the HKLM method is that the non-linear power at $k_{\rm NL}$ derives from the linear power at the smaller $k_{\rm L}$. One would therefore expect that the appropriate treatment for CDM models would be to use a different $f_{\rm NL}$ at each $k_{\rm L}$, according to the tangent spectral index at that point. This is an important assumption, because it means that the small-scale power in CDM models should be representative of the $n<-2$ spectra which are otherwise so hard to treat. Without this assumption, we found our CDM results hard to fit: they reach non-linear powers, on the smallest scales, that are greater than would be expected from even the $n=-2$ power-law fits (see Fig. 4), but the non-linear response at larger scales is less extreme, as would be expected if the effective n were larger. However, although the trend of non-linear response with scale is as expected, the CDM results generally lie below those predicted from the power-law fits using $n_{\rm eff}(k_{\rm L})$. This is not unreasonable: if we compare a CDM spectrum with its tangent power-law spectrum, the power-law spectrum has a greater amount of power when integrating from $k=0$ to $k=k_{\rm L}$. A practical means for accounting for this difference is to conjecture that the non-linear behaviour of the CDM spectrum will be characteristic of its tangent index at some slightly smaller scale, and a shift of a factor of 2 in k gives outstandingly good results:

$$n_{\rm L}(k_{\rm L})\equiv\frac{{\rm d}\ln P}{{\rm d}\ln k}(k=k_{\rm L}/2). \qquad (22)$$

The exact size of the shift is not critical, and we have made no attempt to treat it as an additional parameter to be optimized. Very good predictions of non-linear CDM spectra are achieved even simply using the unshifted tangent spectral index. A shift in this sense is likely to be required for any curved spectrum, where $n_{\rm eff}$ changes slowly with k. Since this prescription clearly also works for pure power-law spectra, we propose this as a general method for dealing with any smoothly curving spectra that are hierarchical in the sense that Δ^2 increases as k increases. The obvious exceptions are therefore spectra with a small-scale cut-off, such as hot or warm dark matter, and these will require separate treatment.

We therefore performed a global fit to the power-law plus CDM data with this assumption, and obtained an excellent fit over all cosmological models, with an rms accuracy of about 14 per cent in $f_{\rm NL}(x)$. This is a demanding level of agreement, since $f_{\rm NL}(x)$ is so steep; the scatter in the transverse direction, which governs the accuracy of power-spectrum reconstruction, is only about 7 per cent. As discussed above, errors in $f_{\rm NL}$ partially normalized themselves away when predicting non-linear power, and this figure of 7 per cent is also the approximate rms accuracy with which this method here will predict $\Delta^2_{\rm NL}$ for a given linear spectrum. The best-fitting parameters are

$$A=0.482(1+n/3)^{-0.947} \qquad (23)$$

$$B=0.226(1+n/3)^{-1.778} \qquad (24)$$

$$\alpha=3.310(1+n/3)^{-0.244} \qquad (25)$$

$$\beta=0.862(1+n/3)^{-0.287} \qquad (26)$$

$$V=11.55(1+n/3)^{-0.423}. \qquad (27)$$

Note once again that the cosmological model does not enter anywhere in these parameters. It is present in the fitting formula only through the growth factor g, which governs the amplitude of the virialized portion of the spectrum. This says that all the quasi-linear features of the power spectrum are independent of the cosmological model, and only know about the overall level of power. This is not surprising to the extent that quasi-linear evolution is well described by the Zeldovich approximation, in which the final positions of particles are obtained by extrapolating their initial displacements by some universal time-dependent factor. All information on the cosmological model is hidden in this extrapolation factor, and therefore the model should have no effect if we scale to displacements of the same size. The power spectrum in the Zeldovich approximation has been calculated analytically by Taylor (1993) and by Schneider & Bartelmann (1995), and it would be of interest to compare their results with ours.

4 DISCUSSION

We have investigated in detail the scaling formula of HKLM for the evolution of clustering statistics in cosmology. Although not completely spectrum-independent, their approach can be made to give a good fit for a variety of spectra, provided one uses a simple dependence on the tangent slope of the linear power spectrum. Because of the need for a spectrum-dependent correction, we have not provided a fitting formula for $\bar{\xi}$, nor for the inverse non-linear function. Inverting observed non-linear data is now in any case an iterative process, and $\bar{\xi}$ is a statistic of less practical interest than the power spectrum. It is probably best to proceed numerically with the forward non-linear function as a starting point.

The main feature of the non-linear HKLM function in this work is a power law on intermediate scales which is rather steep, $f_{\rm NL}(x)\propto x^{1+\alpha}$ with $\alpha\simeq 3.5$–4.5, and it is a challenge to understand this result. Padmanabhan (1996) has given arguments to suggest that the intermediate slope should be $f_{\rm NL}(x)\propto x^3$, but it seems that this is not the true value. For spectra with $n\simeq 0$, such an index works well enough, but this appears to be an artefact of the relatively rapid onset of the virialized regime. For lower densities or very negative n, the virialized regime occurs at larger powers, so that the steeper intermediate behaviour of $f_{\rm NL}(x)$ is seen more clearly. This steep quasi-linear function has an interesting implication for the scaling of small-scale power spectra and their evolution with time. For $\Delta^2\gg 1$, we have

$$k_{\rm NL}\simeq[\Delta^2_{\rm NL}]^{1/3}k_{\rm L} \qquad (28)$$

$$\Delta^2_{\rm NL}\propto[D^2(a)\,\Delta^2_{\rm L}]^{1+\alpha},$$

where $D(a)$ is the linear growth law for density perturbations. For a power-law linear spectrum, this predicts a quasi-linear power law

$$\Delta^2_{\rm NL}\propto D^{(6-2\beta)(1+\alpha)/3}k^{\beta}_{\rm NL}, \qquad (29)$$

where the non-linear power-law index depends, as follows, on the slope of the linear spectrum:

$$\beta=\frac{3(3+n)(1+\alpha)}{3+(3+n)(1+\alpha)}. \qquad (30)$$

For the observed index of $\beta\simeq 1.8$, this would require $n\simeq -2.2$, very different from the $n=0$ that would give $\beta=1.8$ in the virialized regime. However, especially for low-density models, the virialized regime is only reached on very small scales and the observed clustering data are dominated by quasi-linear effects. It is then interesting to note that the predicted evolution is faster than the linear $\Delta^2\propto D^2(a)$; this

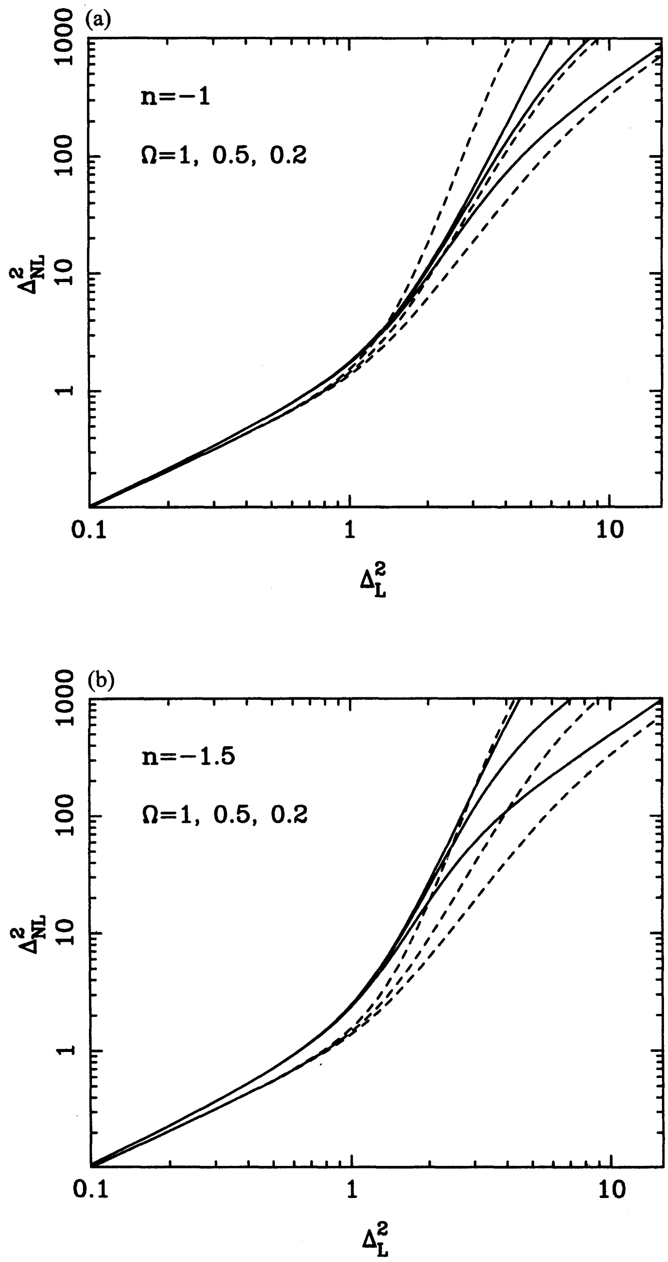

Figure 5. The present fitting formula for the non-linear function (solid lines) compared with the spectrum-independent form suggested by PD (dashed lines), for the cases $n=-1$ and -1.5 and open models with $\Omega_{\rm m}=1$, 0.5 and 0.2. The PD formula was an approximation to the average effect of these different spectra, but the detailed agreement is often poor, particularly at low Ω for flatter spectra. However, these deviations are small in the regime of the data used by PD ($\Delta^2_{\rm NL}\lesssim 3$).

may be of relevance in understanding the weak angular clustering of faint galaxies (e.g. Efstathiou et al. 1991; Roche et al. 1993).

These results should be of practical use for a variety of cosmological investigations. The most obvious case is the theme pursued in PD: linearizing observed clustering data in an attempt to infer the underlying linear power spectrum. The fitting formula used by PD was restricted by the assumption that $f_{\rm NL}$ was spectrum independent, and the results given here are of considerably greater accuracy, particularly for $n \lesssim -1$. How much this matters depends on the application of interest; because $f_{\rm NL}$ is so steep, it is possible to predict $\Delta^2_{\rm NL}$ rather badly and yet be able to infer $\Delta^2_{\rm L}$ with tolerable accuracy. This is illustrated in Fig. 5, which compares the present fitting formula with the one given in PD. There are deviations of up to a power of 10 in $\Delta^2_{\rm NL}$ in the case of great non-linearity and low density. However, in the regime of the data actually used by PD ($\Delta^2_{\rm NL} \lesssim 3$), the errors in the deduced $\Delta^2_{\rm L}$ from a given non-linear power are at most around 20 per cent; the work reported here thus does not imply any serious revision of the conclusions reached in PD. Nevertheless, there remains the challenge of understanding the highly non-linear portion of the power spectrum, and the improved fitting formula from this paper should be of use in attempts to interpret the clustering data in this regime.

ACKNOWLEDGMENTS

SJD was supported by a SERC/PPARC research studentship during part of this work. We salute Hugh Couchman for his tremendous contribution to cosmology in making his AP3M code freely available. We thank Bhuvnesh Jain for helpful correspondence on this subject.

REFERENCES

Baugh C. M., Efstathiou G., 1994, MNRAS, 270, 183
Baugh C. M., Gaztañaga E., Efstathiou G., 1995, MNRAS, 274, 1049
Carroll S. M., Press W. H., Turner E. L., 1992, ARA&A, 30, 499
Couchman H. M. P., 1991, ApJ, 368, L23
Efstathiou G., Bernstein G., Katz N., Tyson T., Guhathakurta P., 1991, ApJ, 380, 47
Hamilton A. J. S., Kumar P., Lu E., Matthews A., 1991, ApJ, 374, L1 (HKLM)
Jain B., Mo H. J., White S. D. M., 1995, MNRAS, 276, L25 (JMW)
Lahav O., Lilje P. B., Primack J. R., Rees M. J., 1991, MNRAS, 251, 128
Padmanabhan T., 1996, MNRAS, 278, L29
Peacock J. A., Dodds S. J., 1994, MNRAS, 267, 1020 (PD)
Peacock J. A., Nicholson D., 1991, MNRAS, 253, 307
Peebles P. J. E., 1980, The Large-Scale Structure of the Universe. Princeton Univ. Press, Princeton, NJ
Roche N., Shanks T., Metcalfe N., Fong R., 1993, MNRAS, 263, 360
Schneider P., Bartelmann M., 1995, MNRAS, 273, 475
Taylor A. N., 1993, in Bouchet F., Lachièze-Rey M., eds, Proc. Cosmic Velocity Fields, 9th IAU Conf. Editions Frontières, Gif-sur-Yvette, p. 585